Eur. Phys. J. B **12**, 157–162 (1999)

THE EUROPEAN PHYSICAL JOURNAL B

EDP Sciences

Non-linear elastic behavior of light fibrous materials

M. Baudequin[a], G. Ryschenkow, and S. Roux

Laboratoire "Surface du Verre et Interfaces"[b], CNRS/Saint-Gobain, 39 Quai Lucien Lefranc, 93303 Aubervilliers Cedex, France

Received 2 February 1999

Abstract. Light fibrous materials composed of elastic fibers display a non-linear elastic behavior, where the non-linearity is due to the increase in the number of contacts between fibers under compression. Testing glass wool under compression up to 95% shows such a strongly non-linear behavior. A model is proposed to account for the divergence of the compressive stress σ as the strain ε approaches a threshold compression ε^*, with $\sigma \propto (\varepsilon^* - \varepsilon)^{-3/2}$. Quantitative analysis of the experimental data on glass wool is fully consistent with this result.

PACS. 62.20.-x Mechanical properties of solids – 62.20.Dc Elasticity, elastic constants

1 Introduction

Light fibrous materials generally present an extremely low apparent density and hence are good candidates for their performance as thermal insulating materials. This is indeed the case for glass wool which is the material we will use below to illustrate our model. This low density also encourages one to store these materials under a high compression and hence, this requires a good understanding of their mechanical properties under large compressive strains. In the case of glass wool, the typical compression is about 90 to 95 % [1].

Under such large strains, the behavior of glass wool is no longer linearly elastic but (after of few strain cycles) it can still remain elastic (friction, damage, visco-elastic effects can be ignored for a first order description). The most obvious origin of this non-linearity is the creation of contacts between fibers.

The most famous example of such a non-linearity is the Hertz problem describing one single elastic contact between two solids, and where the force displacement relation is not linear because of the variation of the contact area as the contact force is changing [2]. In the case of glass wool, in contrast, contacts are created inside the bulk of the material.

The literature is rather limited on such a subject. In the study of the geometry of fibrous materials, some information can be found on the packing fraction of *rigid* rods, taking into account either a hard-core repulsion or allowing for some overlap between rods [3,4]. The interest on this question arouse because of the applicability of this concept to the study of conductivity properties of composites reinforced with short fibers [5]. However, because of the rigidity of the rods which is postulated in those studies, it is difficult to extend the obtained results to deformable fibers such encountered in glass wool.

Going beyond the pure geometrical problem, analogies can be searched for in low density materials, such as foams, composites, or other generically cellular materials whose properties have been reviewed extensively by Gibson and Ashby [6]. However, here again, many other aspects may come into play in the mechanical behavior of these materials. In particular when large deformations are reached, either damage, crushing, or simply elastic buckling must be considered, and for contact non-linearity to be dominant, severe constraints are imposed on the constituents of the materials. Most studies thus did not observe a non-linear elastic behavior in the so-called "densification regime", which could be attributed mainly to contacts.

An analogy in two dimensions can be found in a recent study by Sherwood and Vandamme [7] which addressed the mechanical behavior of clays through a model systems consisting in rectangular platelets held between two parallel glass plates through which the densification could be observed at the level of individual contacts. Such a system does respond elastically in a large range of strain, and most of the non-linearity comes from contacts being created. However because of the two-dimensional nature of the problem, contacts are established along large segments of the platelets and thus the nature of these contact is quite different from our fibrous systems.

2 Model

The geometry of the material is a loose array of fibers interconnected at contacts (*cf.* Fig. 1). Thus there are two very different scales: one is the fiber diameter d, and the other is the mean distance between contact points $\langle \ell \rangle$. The former remains constant and it controls the elastic

[a] e-mail: maud.baudequin@sgr.saint-gobain.com
[b] UMR 125 CNRS/Saint-Gobain

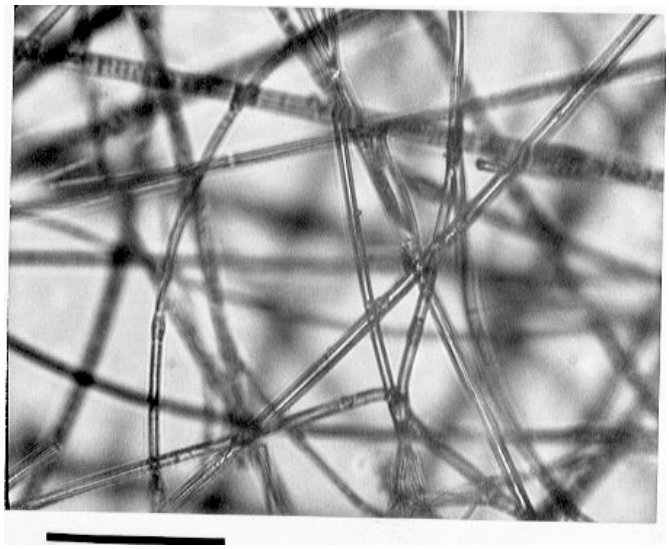

Fig. 1. Optical photomicrography by transmission showing a typical texture of a layer sampled from glass wool used in the experimental part enclosed between two glass plates. Scale bar represents 100μm.

properties of the fibers, whereas the latter changes as the sample is compressed. A reasonable approximation when the material remains loose, is to approximate the fibers by arcs, describing them using curvilinear elasticity, where only flexion is considered. Thus the only remaining length scale is the distance between contacts.

As a consequence, different geometries of the fiber network for different levels of stress can be related by a simple scale transformation. Let us show that this simple observation already implies a power-law relation between ℓ and the stress, σ. Let us imagine changing the stress from σ to $\sigma' = a\sigma$. Due to the absence of any other length scale, there exists a scale factor depending on a, $f(a)$ relating the intercontact distance in those two cases, $\ell' = f(a)\ell$. If we now perform a second consecutive transformation, to $\sigma'' = b\sigma'$, then $\ell'' = f(b)\ell'$. One could also consider going from σ to σ'' and $\ell'' = f(ab)\ell$. This implies

$$f(ab) = f(a)f(b) \tag{1}$$

for all values of a and b. This group property implies that f is a power-law. This can be easily retrieved by differentiating the above equation with respect to b:

$$af'(ab) = f(a)f'(b) \tag{2}$$

and setting $b = 1$:

$$\frac{f'(a)}{f(a)} = \frac{\mu}{a} \tag{3}$$

where $\mu = f'(1)$. Integration of this differential equation leads to

$$f(a) = a^{\mu} \tag{4}$$

where we have used the condition $f(1) = 1$ (no stress change implies no scale change) to set the prefactor. If this argument justifies the existence of a power-law relation between σ and ℓ, $\ell \propto \sigma^{\mu}$, it cannot provide the value of the exponent.

This section is devoted to an explicitly derivation of such a scale transformation. First we will relate stress and strain at a macroscopic level to forces and displacements between contact points, using dimensional arguments. Then we will obtain the scaling of the distance $\langle \ell \rangle$ with the compression stress. These results will give the stress strain relationship in the elastic regime.

2.1 From microscopic to macroscopic

In this subsection, we will ignore the statistical distribution of distances ℓ between contact points, and treat ℓ as a fixed value for a given stress.

We assume that the fibers obey linear elasticity over the full range of strain. However, the macroscopic stress-strain relation being non-linear, we consider only an infinitesimal increment of stress $d\sigma$ around an equilibrium state.

Fibers are subjected to forces F and torques M. We ignore fiber elongation or compression due to these forces, and focus on flexural torques M ($\ell \gg d$). There exists several contact points in a layer of fibers. For each state of compression, the mean number of these contact points by surface unit is $1/\ell^2$. Thus the increment of stress gives rise to an increase of forces being transmitted at contacts of order

$$\frac{1}{\ell^2}\mathrm{d}F = \mathrm{d}\sigma. \tag{5}$$

Curvilinear elasticity [8] gives the flexural stiffness k of a fiber as a function of its length (we ignore the dependence on d because we assume a narrow distribution of fibers diameters)

$$k \propto \ell^{-3}. \tag{6}$$

We do not take account the dependence of k on other properties of the fiber (diameter or Young's modulus because they are not varying during the mechanical test). The apparent coefficient of Poisson is nil and therefore the average relative displacement is (on average) parallel to the direction of compression. We note $U = \|\mathbf{U}\|$. The relative displacement U of neighboring contact points thus increases as

$$\mathrm{d}U \propto k^{-1}\mathrm{d}F \propto \ell^5 \mathrm{d}\sigma. \tag{7}$$

Let us introduce h_0 the initial thickness of the sample supporting no stress, and h its current thickness. The change of thickness dh, resulting from the stress increment, is given by the relative displacement between contact points dU times the number of contacts along a continuous directed path across the sample. This number is in fact a property which directly result from the structure of the fiber orientation and arrangement in the wool. In the case of a strong layering of fibers in plane perpendicular to the compression axis, we assume here that the number of contacts along a continuous directed path across the sample is fixed. Therefore

$$\mathrm{d}h \propto \ell^5 \mathrm{d}\sigma. \tag{8}$$

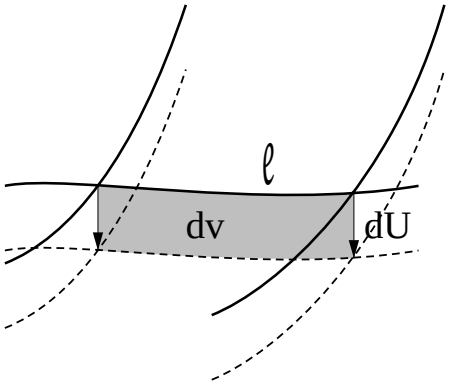

Fig. 2. Sketch of the volume of space, dv, swept by a fiber portion, ℓ, during an increment of displacement, dU.

For large strains, there are different ways of defining the strain. We choose by convention to define the strain as the relative reduction of height of the sample under compression, $\varepsilon = \delta h/h_0$. Hence

$$\mathrm{d}\varepsilon \propto \ell^5 \mathrm{d}\sigma. \tag{9}$$

The above equations allow to relate the macroscopic variables to the microscopic ones. There remains to determine the evolution of ℓ as a function of σ.

2.2 Distance between contact points

In contrast to the previous section, we introduce the statistical distribution of distances between contacts denoted through $n(\ell, \sigma)$. We will write down the evolution of this distribution as the stress increases. For simplicity, we will call a "bond" the fiber segment between two consecutive contacts.

For this we need to know the probability $p(\ell, \sigma)\mathrm{d}\sigma$ that in a small stress increment dσ, a bond of length ℓ encounters another fiber and thus creates a new contact. The volume of space swept by this bond in the stress increment dσ is dv (*cf.* Fig. 2). Once again ignoring constant factors such as the fiber diameter, this volume scales as

$$\mathrm{d}v \propto \ell \mathrm{d}U \propto \ell^6 \mathrm{d}\sigma. \tag{10}$$

Due to the absence of stress scale, we argue that the probability p is simply proportional to the swept volume for a fixed *relative* stress increment

$$p(\ell, \sigma)\frac{\mathrm{d}\sigma}{\sigma} \propto \mathrm{d}v \tag{11}$$

or

$$p(\ell, \sigma) = \varpi \ell^6 \sigma \tag{12}$$

where ϖ is a constant.

There are three contributions to the evolution of the number of bonds in the stress increment dσ: a fraction $n(\ell, \sigma)\mathrm{d}\ell$ will establish a new contact with a probability $p(\ell, \sigma)\mathrm{d}\sigma$. Those bonds will disappear from the initial population. Similarly longer bonds of length ℓ' will create a new contact which may give rise one bond of length ℓ and a second one length $\ell' - \ell$. We assume that a new contact may be created anywhere on the original bond. The number of bonds which are susceptible to create such contacts is $n(\ell', \sigma)$. The probability of these events is $q(\ell' \to \ell)$ and $q(\ell' \to \ell' - \ell)$. The balance equation for those bonds reads

$$\frac{\mathrm{d}n(\ell, \sigma)}{\mathrm{d}\sigma} = -n(\ell, \sigma)p(\ell, \sigma) + \int_\ell^\infty n(\ell', \sigma)q(\ell' \to \ell)\mathrm{d}\ell' + \int_\ell^\infty n(\ell', \sigma)q(\ell' \to \ell' - \ell)\mathrm{d}\ell'. \tag{13}$$

We can write

$$q(\ell' \to \ell) = p(\ell', \sigma)\psi(\frac{\ell}{\ell'})\mathrm{d}\frac{\ell}{\ell'} \tag{14}$$

and

$$q(\ell' \to \ell' - \ell) = p(\ell', \sigma)\psi(1 - \frac{\ell}{\ell'})\mathrm{d}\frac{\ell}{\ell'} \tag{15}$$

where ℓ/ℓ' is a random variable varying between 0 and 1 and ψ the uniform distribution between 0 and 1.

But $\psi(\ell/\ell') = \psi(1 - \ell/\ell')$ because the problem is symmetrical. Then

$$\frac{\mathrm{d}n(\ell, \sigma)}{\mathrm{d}\sigma} = -n(\ell, \sigma)p(\ell, \sigma) + 2\int_\ell^\infty n(\ell', \sigma)p(\ell', \sigma)\frac{\mathrm{d}\ell'}{\ell'}. \tag{16}$$

Similar equations are encountered in modeling of fragmentation [9]. Without solving exactly the above equation, two strategies lead to the scaling of ℓ with the stress. Both are clarified in the following subsections.

2.3 Analysis of moments

Let us introduce the moment of the bond length of order k as

$$M_k \equiv \int_0^\infty n(\ell, \sigma)\ell^k \mathrm{d}\ell. \tag{17}$$

Integration of the balance equation (Eq. (16)) leads to the following recurrence

$$\frac{\mathrm{d}M_k}{\mathrm{d}\sigma} = \varpi\sigma\left(\frac{2}{k+1} - 1\right)M_{k+6}. \tag{18}$$

Only one of these equations is directly integrable ($k = 1$), but it gives only a trivial result, namely that the total fiber length remains constant (independent from σ). Other moments scale with the stress according to

$$M_k(\sigma) = A_k \sigma^{\zeta(k)} \tag{19}$$

where the prefactors A_k are related to each other through recurrence relations which are not clarified here since we will not exploit them any further. From equation (18), we obtain:

$$\zeta(k) = \zeta(k+6) + 2 \tag{20}$$

and the fact that M_1 is constant give $\alpha(1) = 0$. The general solution of equation (20) is $\zeta(k) = (1-k)/3 + \gamma(k)$ where $\gamma(k)$ obeys $\gamma(1) = 0$ and $\gamma(k+6) = \gamma(k)$ *i.e.* γ is periodic of period six. The exponents $\zeta(k)$ govern the scaling of different moments of the distribution and thus they obey convexity properties, $\partial^2\zeta(k)/\partial k^2 = \partial^2\gamma(k)/\partial k^2 \geq 0$, which imply $\gamma(k) = 0$, hence

$$\zeta(k) = \frac{(1-k)}{3}. \tag{21}$$

The above scaling can be physically understood as follows: the total number of bonds is given by M_0 and it increases as $\sigma^{1/3}$. A typical length of a bond can be defined through the ratio of two consecutive moments, *e.g.* $\ell \propto M_{k+1}/M_k$. One of these is the average bond length, $\langle\ell\rangle = M_1/M_0$. All these ratio behave similarly, as

$$\langle\ell\rangle \sim \sigma^{-1/3}. \tag{22}$$

The above scaling law for the moments simply means that $M_k \approx M_0\langle\ell\rangle^k$, so that in terms of scaling, one may ignore the statistical distribution of ℓ, and use a typical value instead.

2.4 Equivalent derivation from scaling

Instead of studying moments of the distribution as done previously, it is also possible to postulate that the number of bonds of length ℓ for a compressive stress σ is a unique function of the ratio of ℓ over a characteristic length ℓ^* which itself depends on σ. Since the fiber diameter is considered irrelevant, ℓ^* has to be a homogeneous function of σ

$$\ell^* \propto \sigma^{-b}. \tag{23}$$

Hence our scaling hypothesis is

$$n(\ell,\sigma) = \sigma^a\varphi(\ell\sigma^b) \tag{24}$$

where a and b are exponents to be determined, and φ is the scaling function.

Let us introduce $\lambda = \ell\sigma^b$. Substituting the scaling form of n in equation (16) gives

$$a\varphi(\lambda)+b\lambda\varphi'(\lambda) = -\varpi\ell^6\sigma^2\varphi(\lambda)+2\varpi\sigma^2\int_\ell^\infty \varphi(\ell'\sigma^b)\ell'^5\mathrm{d}\ell'. \tag{25}$$

The left hand side of the above equation only depends on λ, thus so must do the right hand side. This determines

$$b = \frac{1}{3} \tag{26}$$

in agreement with the previously derived value. The a exponent can still assume any value. It is determined from the first moment (the total fiber length is stress independent).

$$M_1 = \int \sigma^a\varphi(\ell\sigma^b)\ell\mathrm{d}\ell = \sigma^{a-2b}\int\varphi(u)u\mathrm{d}u \tag{27}$$

thus

$$a = 2b \tag{28}$$

thus

$$n(\ell,\sigma) = \sigma^{2/3}\varphi(\ell\sigma^{1/3}). \tag{29}$$

Finally using these values, we arrive at the equation to be solved for the scaling function φ

$$\frac{2}{3}\varphi(\lambda)+\frac{\lambda}{3}\varphi'(\lambda) = \varpi\left[-\lambda^6\varphi(\lambda)+2\int_\lambda^\infty\varphi(\lambda')\lambda'^5\mathrm{d}\lambda'\right]. \tag{30}$$

We set

$$\chi(\lambda) = \int_\lambda^\infty\varphi(\lambda')\lambda'^5\mathrm{d}\lambda'. \tag{31}$$

Then $\chi'(\lambda) = \varphi(\lambda)\lambda^5$ and

$$\varphi'(\lambda) = \frac{\chi''(\lambda)}{\lambda^5} - \frac{5\chi'(\lambda)}{\lambda^6}. \tag{32}$$

We obtain

$$\chi''(\lambda)+3\left(\varpi\lambda^5-\frac{1}{\lambda}\right)\chi'(\lambda)-6\varpi\lambda^4\chi(\lambda) = 0. \tag{33}$$

This equation is difficult to solve. The asymptotic behavior can however be obtained for large λ. In this case, one expects φ to decay rapidly. Integration for large λ gives

$$\chi(\lambda) = K_1\lambda^{-4}\left(1+\frac{16}{9\varpi}\lambda^{-6}+\mathcal{O}(\lambda^{-12})\right)\exp\left(-\frac{\varpi\lambda^6}{2}\right) \tag{34}$$

where K_1 is a constant, and then

$$\varphi(\lambda) = K_1\lambda^{-4}\left(-3\varpi+\frac{4}{3}\lambda^{-6}+\mathcal{O}(\lambda^{-12})\right)\exp\left(-\frac{\varpi\lambda^6}{2}\right) \tag{35}$$

i.e. a very abrupt decay to 0, which legitimates a similar scaling of all moments of the distribution.

2.5 Non-linear elastic behavior

With the scaling of ℓ with σ, we now are in position to conclude on the elastic stiffness of the material. Using equation (9), we arrive at a tangent elastic modulus K

$$\frac{\mathrm{d}\sigma}{\mathrm{d}\varepsilon} = K \propto \ell^{-5} \propto \sigma^{5/3}. \tag{36}$$

Integrating this differential equation yields

$$\sigma \propto (\varepsilon^* - \varepsilon)^{-\delta} \tag{37}$$

where

$$\delta = \frac{3}{2}. \tag{38}$$

Thus the stress has been found to diverge for a finite strain ε^*. It should be emphasized that albeit such a divergence is obviously expected from stearic hindrance effects, the latter are not directly at play here since we have considered that the diameter of the fibers is zero. Therefore

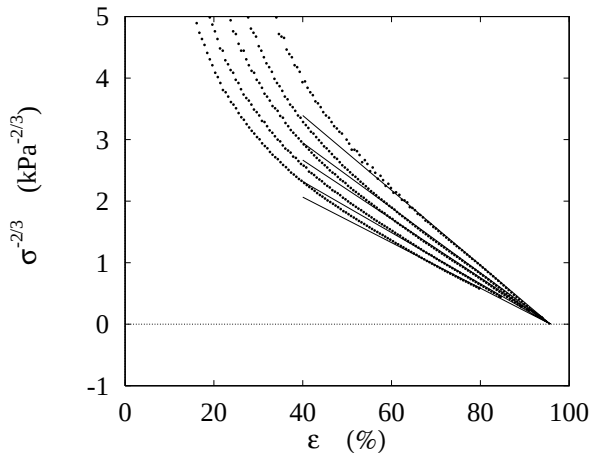

Fig. 3. Non-linear elastic behavior analyzed according to the expected power-law behavior of the theoretical section. Each data set (dots) corresponds to a different imposed strain ε_1 applied prior to recording the present data points ($\varepsilon_1 = 0.95$, 0.92, 0.90, 0.85 and 0.80 respectively from top to bottom). Linear fits are shown as thin lines.

the stearic limitation corresponds to a singular behavior of the stress as the strain reaches 100%. Here the mechanism for the divergence is slightly different. It corresponds to a vanishing of the bond length and hence a divergence of the stiffness. No specific threshold strain was introduced. It appeared from the integration. Moreover the above argument gives the exponent δ of the divergence.

It is important to note that the mean contact force is not directly proportional to the external stress because of the new contacts being created. Indeed we have seen above that $\mathrm{d}F \propto \ell^2 \mathrm{d}\sigma$, or

$$\mathrm{d}F \propto \sigma^{-2/3} \mathrm{d}\sigma \tag{39}$$

thus

$$F \propto \sigma^{1/3} \tag{40}$$

i.e. a much slower increase than naively expected.

Summarizing the above results we can write as a function of strain

$$\begin{cases} \sigma & \propto (\varepsilon^* - \varepsilon)^{-3/2} \\ K & \propto (\varepsilon^* - \varepsilon)^{-5/2} \\ \langle \ell \rangle & \propto (\varepsilon^* - \varepsilon)^{1/2} \\ F & \propto (\varepsilon^* - \varepsilon)^{-1/2} \end{cases} \tag{41}$$

or as a function of the stress

$$\begin{cases} (\varepsilon^* - \varepsilon) & \propto \sigma^{-2/3} \\ K & \propto \sigma^{5/3} \\ \langle \ell \rangle & \propto \sigma^{-1/3} \\ F & \propto \sigma^{1/3}. \end{cases} \tag{42}$$

3 Comparison with experiment

We now turn to the experimental part. The material used was a low density glass wool, produced on a pilot line for research and development purposes. There exists a scattering of diameters of fibers and the average diameter is equal to 4 μm. The wool porosity is approximately equal to 99.6 %.

Although we focus here on the elastic behavior, there are a number of other effects which come into play under compression. Fibers may break inducing damage, they relax when subjected to a steady compression, solid friction may be active at the contacts... Therefore, we performed the following test in order to extract the elastic behavior. A large strain ε_1 was first imposed, and then released. This first loading gives rise to some damage *i.e.* breaking of fibers which reduces the elastic stiffness of the material. However this damage only depends on the maximum compression applied in the past. The first loading curve is thus discarded. A second compression is applied up to ε_1. This second loading phase is the one which is analyzed. No further damage is expected to happen because of the first compression. Friction certainly exists but it should not affect the test as long as the load is not reversed, and thus we did not analyze the unloading.

Parallelepipedic samples of 200×200 mm cross-section have been used. Their height was that of the material as it comes out of the production line (about 130 mm). The wool was freshly produced before the test, but it was not preserved from humidity in any manner. All tests were performed at ambient temperature, and no aging was observed.

Two mechanical testing machine have been used to characterize the behavior of the samples. Constant strain rates $\dot{\varepsilon}$ in the range 4×10^{-3} s^{-1} to 4×10^{-2} s^{-1} were imposed for the compression and the unloading. No significant differences could be noted as a function of strain rate.

The behavior was analyzed by plotting the stress raised to the power $-1/\delta = -2/3$ as a function of the strain. Figure 3 shows such plots for five different ε_1, (0.95, 0.92, 0.90, 0.85, 0.80 from top to bottom), and the corresponding linear fits.

The first feature revealed by this graph is that the power-law divergence seems to be well obeyed. No curvature in the data points is visible for large strains. Second, we note that the compression curves are significantly dependent on ε_1. This is to be interpreted as damage taking place in the sample as the maximum imposed strain increases. Third, amazingly the point of divergence ε^* appears to be independent of ε_1. This may be due to the fact that as fibers are broken, they mostly remain in place and thus broken fibers may still be brought to contact and thus they do not affect the maximum compaction. From the fits, we estimate

$$\varepsilon^* \approx 0.96 \tag{43}$$

i.e. just one percent above the largest imposed strain.

For small to moderate strains, the power-law relation between stress and strain is not obeyed. In fact, a binder is sprayed on the glass wool at the final stage of manufacturing, to give it better mechanical performances. This binder establishes permanent connections between fibers.

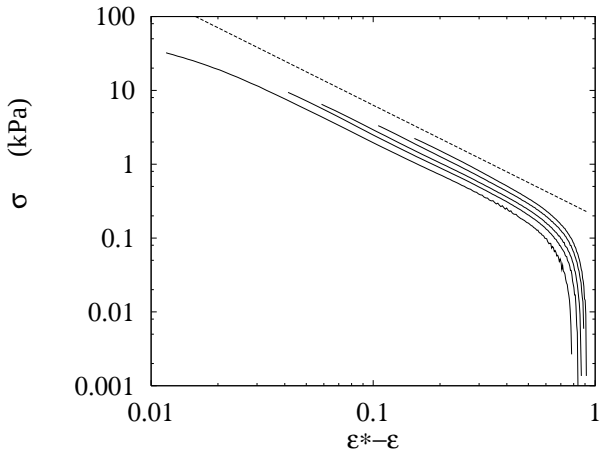

Fig. 4. Same data as the previous figure in log-log coordinates. The different curves refer to different levels of maximum strain applied to the material (and hence different damage levels). From up to the bottom, the maximum strain applied decrease. We note that the same value of ε^* has been used in this plot for all data sets. The dotted line indicates a slope of $-3/2$.

Indeed it is observed that for strains less than about 30%, the behavior is simply linear elastic. In this regime, the elastic behavior is very little governed by the creation of new contacts, but by the mean distance between chemically glued fiber connections. Then, for larger strains, new contacts begin to contribute to the non-linear elastic behavior. This regime is accurately followed only for strains larger than about 60%.

Figure 4 shows on a log-log scale the evolution of σ *versus* the strain difference $\varepsilon^* - \varepsilon$ for various damage levels. A straight line of slope -3/2 is shown as a guide to the eye. We do observe that the power-law regime is indeed very accurately reproduced and is fully consistent with the previous analysis. This second graph however magnifies the strains close to ε^*, and still do not reveal any systematic deviations. Finally, we estimate $\delta = 1.5 \pm 0.1$ in excellent agreement with the theoretical value.

The figures shown here are only examples of such a behavior. Many other experiments have been performed with other samples at different loading velocities, with different loading histories, and similar results have been obtained consistently, provided damage is avoided in the analyzed data by a prior loading.

4 Conclusion

The main purpose of the present investigation was to study the elastic behavior of a light fibrous material and particularly the divergence of the compressive stress, σ, as the strain approaches the critical compression ε^*. To describe the non-linear elastic behavior, we propose the law $\sigma \propto (\varepsilon^* - \varepsilon)^{-3/2}$ where ε^* is an intrinsic property of the material, independent of its damage. The broken fibers do not affect the divergence strain, ε^*, because these fibers still contribute to contacts during compression. This law was theoretically justified, and many experiments have been performed and have confirmed the validity of our description.

It is worth emphasizing that in spite of the variability of the samples density, thickness or distribution of binding agent, the above non-linear elastic behavior appears to be extremely robust and in particular the 3/2 exponent is very accurately measured on all samples.

We have not studied mechanical properties like damage (breaking of fiber), viscoelastic effects and friction. The latter have to be considered in order to reach a more accurate macroscopic description of the mechanical behavior of light fibrous materials, but they clearly fall outside the scope of the present study.

To study the non-linear elastic behavior, we have assumed that the mechanical behavior of the fibers was linear elastic and that the only source of non-linearity was due to the geometry of contacts, *i.e.* the increase in the number of contacts between fibers during compression. Let us note that a similar treatment may be applied to the viscoelastic behavior. This opens the way to describe the apparent non-linear viscoelastic behavior of these materials consistently. Future work is planned in this direction.

We wish to thank D. Bideau et R. Blanc for their contribution to this study. We are grateful to C. Langlais, M.H. Rouillon and G. Levasseur for useful discussions and suggestions about the present work. This work has been fully supported by the "Centre de Recherches Industrielles de Rantigny" of Isover Saint-Gobain.

References

1. C. Langlais, S. Klarsfeld, Technique de l'Ingénieur, *Isolation thermique à température ambiante*, **B2II**, BE 9861 (1998).
2. K.L. Johnson, *Contact Mechanics* (Cambridge University Press, 1985).
3. A.L.R. Bug, S.A. Safran, I. Webman, *Continuum percolation of rods*, Phys. Rev. Lett. **54**, 1412-1415, (1985).
4. I. Balberg, N. Binenbaum, N. Wagner, *Percolation thresholds in the three dimensional sticks system*, Phys. Rev. Lett. **52**, 1465-1468, (1984).
5. F. Carmona, F. Barreau, R. Canet, P. Delhaes, *An experimental model for studying the effect of anisotropy on percolative conduction*, J. Phys. Lett. **41**, 534, (1980).
6. L.J. Gibson, M.F. Ashby, *Cellular Solids* (Pergamon Press, Oxford, 1988).
7. J.D. Sherwood, H. Vandamme, *Non-linear compaction of an assembly of highly deformable platelike particles*, Phys. Rev. E **50**, 3834-3840, (1994).
8. S. Timoshenkow, J.N. Goodier, *Theory of elasticity* (Mc Graw-Hill, New York, 1951).
9. S. Redner, *in Statistical models for the fracture of disordered media*, edited by H. Herrmann, S. Roux, (North-Holland, Amsterdam, 1990), Chap. 10, p. 321.